



Universidad
Carlos III de Madrid



This is a postprint version of the following published document:

Paredes, E.C. (et al.) *Influence of the forming process of corrugated stainless steels on their corrosion behaviour in simulated pore solutions*. En: *Corrosion Science* 58 (May 2012), pp. 52-61. DOI: [10.1016/i.corsci.2012.01.010](https://doi.org/10.1016/i.corsci.2012.01.010)

© 2012 Elsevier Ltd.



This work is licensed under a Creative Commons Attribution-NonCommercial-NoDerivatives 4.0 International License.

Influence of the forming process of corrugated stainless steels on their corrosion behaviour in simulated pore solutions

E.C. Paredes, A. Bautista*, S.M. Alvarez, F. Velasco

Material Science and Engineering Department – I.A.A.B., Universidad Carlos III de Madrid, Avda. Universidad 30, Leganés, Madrid, Spain

A B S T R A C T

Stainless steels are formed by either hot working (HW) or cold working (CW) when used as reinforcement for concrete structures. The influence of the forming process on the corrosion behaviour is analyzed in depth in the present work. CW and HW corrugated bars of austenitic AISI 304L and 316L, and duplex SAF 2205 grades are studied. The electrochemical behaviour of the corrugated surface and the core of these materials are characterized by Mott Schottky analysis and polarization curves. Tests are carried out in both carbonated and non carbonated $\text{Ca}(\text{OH})_2$ solutions. The microstructure and local mechanical properties of these materials are also analysed by means of universal hardness (UH) measurements to complete available information. The results prove that the surface of corrugated bars is far more likely to suffer corrosion than the core of the same material. The corrosion probability and the morphology of the attack induced in corrugated surfaces by anodic polarization clearly differ in HW and CW bars.

Keywords:

- A. Stainless steel
- A. Steel reinforced concrete
- B. Polarization
- C. Effects of strain
- C. Pitting corrosion
- C. Hardening

1. Introduction

The corrosion resistance of stainless steel in mortars or concrete is much higher than that of the carbon steel traditionally used as reinforcement [1–4]. Simulations of chloride penetration into concrete exposed to periodic de-icing salts predict that the time until corrosion initiation may increase 100 years or more for concrete structures when stainless steel reinforcements replace carbon steel [5].

A problem initially posed by the use of stainless steel reinforcements was that these materials must meet the mechanic requirements offered by carbon steel in terms of yield strength, stiffness and ductility, so as carbon steel can be easily substituted as structural material [6]. Stainless steels are typically softer than carbon steel. A simple stainless steel cladding of carbon steel bars proves very sensitive to surface defects in the material [5]. From the view point of corrosion, the most reliable option is the application of a specially designed hardening treatment. Although this treatment makes the product somewhat more expensive, it provides stainless steels with the appropriate mechanic features. Reinforcements of different types of both cold worked (CW) and hot worked (HW) stainless steels can be currently found in market. CW is usually employed for bar diameters over 11–12 mm, while HW is more appropriate for higher diameter bars.

Some studies analyse the influence of processing on the tensile results of corrugated stainless steels [7]. The presence of

corrugations was observed to modify the tensile properties and the fatigue behaviour of stainless steel. Worse results are obtained when testing stainless steel bars with corrugations than when they are eliminated [8].

Regarding the corrosion behaviour of stainless steel in concrete, their performance was proven to depend on the pH and composition of the pore solution. As expected, chloride concentration leads to increase the risk of pitting corrosion in stainless steel [9–13]. Most authors also agree in the fact that higher alkalinity in the pore solution has a positive impact on the corrosion behaviour of stainless steel [10–13]. The influence of the alloying elements in base metal on the corrosion behaviour in simulated pore solutions was also studied [10–15], as well as the influence of scales on stainless steel surface [5,11,16]. However, no deep study on the possible influence of the processing method, and thus, of the microstructure, on the corrosion behaviour of corrugated stainless steel could be found in literature.

Studies carried out in neutral and acidic conditions show up a likely relationship between mechanical hardening induced in stainless steels and their pitting behaviour [17,18]. Pit development in stainless steels is postulated to depend on metallurgical factors such as stresses, density of dislocations, and preferential orientation of the crystallographic planes. It has been proven that the influence of the forming process on pitting can change with the stainless steel composition and the pH and contaminants in the environment [19].

Pitting has also been previously related to the stoichiometric characteristics of the passive layers. The stoichiometry of passive layers on stainless steels has been previously evaluated using Mott Schottky analysis [20]. This approach allows to obtain

* Corresponding author. Tel.: +34 916249914; fax: +34 916249430.

E-mail addresses: asuncion.bautista@uc3m.es, mbautista@ing.uc3m.es (A. Bautista).

information about the type of stoichiometric deviation of the oxide that form the passive layer under different circumstances, as well as to quantify the amount of defects. Recent results prove that stoichiometry of the passive layers in stainless steels is modified by the pH [21,22], oxidation temperature or the formation potential [23]. The ability of the method for detecting changes in the passive layers due to the forming process has not been checked up to now. Hence, it is interesting to evaluate how the forming processes of stainless steel reinforcements can affect the characteristics of the passive layers and the corrosion behaviour in concrete.

There are some experimental evidences seem to prove that corrosion always appear on corrugations when the real surface of the stainless steel reinforcements is tested [10,12]. However, a great amount of the recently published work on stainless steel corrosion performance in simulated pore solutions used polished sections of stainless steels embedded in resin [5,7,9,13,24–26], and sometimes the samples had been cut from stainless steels that had not been processed as corrugated bars [27–30]. In these cases, the possible influence of the forming method and the characteristic microstructure of the corrugations were not considered. Though corrosion tests were carried out on the real surface of the reinforcements in some studies [5,10,12,16], the possible influence of the forming process on the pitting resistance of the material and on the corrosion mechanism was not analysed.

The aim of the present paper is to use different techniques of obtain new information about how the forming process can affect the corrosion behaviour of stainless steels in simulated pore solutions. With this objective, results obtained with HW and CW bars of similar chemical composition are analyzed and compared with results obtained for samples of the core of the bars.

2. Experimental procedure

Three different stainless steel grades were considered in this study: AISI 304L, AISI 316L and SAF 2205. These grades were selected because of their current market importance. Their characteristics and corrosion performance were analysed when manufactured by both HW and CW. All the corrugated bars were processed by the Spanish manufacture company Roldán S.A. (ACERINOX Group). The diameters and chemical compositions of the six corrugated stainless steel grades are shown in Table 1.

The tensile properties of the corrugated stainless steels can be seen in Table 2. It is noteworthy mentioning that the yield strength of the HW corrugated bars double that of materials with the same composition processed by CW for other more traditional applications [31]. The usual information about the mechanical properties of the bars obtained from tensile tests was supplemented with the more localized studies carried out through universal hardness (UH)

Table 2

Tensile mechanical properties of the corrugated stainless steels considered in the study.

	AISI 304L		AISI 316L		SAF 2205	
	CW	HW	CW	HW	CW	HW
YS (MPa)	580	580	656	603	968	583
UTS (MPa)	747	780	822	800	1156	855
Elongation (%)	38	15	26	12	12	33

measurements. Results were obtained on cross sectional, metallographically prepared samples of the bars. Measurements were carried out on the corrugation and at the centre of the bars. Tests were performed at a load rate of 1 mm/min using a maximum load of 20 N. UH plastic hardness, indentation modulus, and mechanical work (together with the elastic and plastic parts of the indentation work) were measured. Microhardness was measured at the same time in each point. All results are the average of about 15 measurements. Some theoretical background about this characterization method can be found elsewhere [32].

The microstructural study of stainless steels was carried out on cross sections of the corrugated bars. Metallographically prepared specimens were chemically etched to reveal their microstructure. For austenitic stainless steels, *aqua regia* (HCl + HNO₃ solution) was used as a reagent agent, while the Bloech and Wedl reactive (HCl + K₂S₂O₅ solution) was used for duplex grades. Grain size in stainless steel was measured on the bulk of the bars and on the corrugation according to the ASTM E112 standard.

Electrochemical polarization studies were carried out on the corrugated surface of stainless steel reinforcing bars. A 2 cm long surface area of the bars was immersed in the test solution. Neither the microstructure of the corrugated surface nor the usual industrial passivating treatment were modified. The influence of the industrial passivating treatment on the protecting nature of the passive layer had already been suggested in the bibliography [14]. The cross section of the bars was also exposed to the solution, although it had been previously ground to 320 and passivated (50 s in 12% HNO₃ (w/w)). Experimental evidence demonstrates that the attack never localizes in the cross section, so the measurement of the length of the passive region obtained under these conditions always corresponds to that of the corrugated surface. No risk of differential aeration corrosion exists for corrugated stainless steels in alkaline media with this cell configuration.

Materials were polarized in eight different simulated pore solutions at room temperature. Fresh, saturated Ca(OH)₂ solutions (pH ≈ 12–13) were used to simulate non carbonated concrete. Solutions where the pH had been reduced to about nine by bubbling CO₂ enriched air were used to simulate carbonated concrete.

Table 1

Nominal diameter and chemical composition of the six corrugated stainless steels considered in the study.

	AISI 304L		AISI 316L		SAF 2205	
	CW	HW	CW	HW	CW	HW
Diameter (mm)	12	16	6	16	12	20
<i>Chemical composition (% w/w)</i>						
C	0.023	0.026	0.018	0.013	0.029	0.020
P	0.031	0.027	0.03	0.029	0.029	0.018
S	0.001	0.001	0.002	0.003	0.001	0.003
Si	0.361	0.298	0.365	0.351	0.387	0.374
Mn	1.448	1.420	1.441	1.782	1.721	1.665
Cr	18.30	18.37	16.97	16.76	22.49	22.17
Ni	8.675	8.740	11.21	11.17	4.721	4.710
Mo	0.275	0.275	2.081	2.504	3.221	3.500
N	0.0507	0.0549	0.0476	0.0443	0.1743	0.1778
Cu	0.487	0.506	0.497	0.257	0.237	0.093
Fe	Bal.	Bal.	Bal.	Bal.	Bal.	Bal.

At both pHs, tests were carried out in solutions without chlorides and with three different amounts of NaCl (0.5%, 1% or 5% (w/w)). Polarization curves were performed after 17 h of exposure of the reinforcements to the simulated pore solutions, as meaningful change in passive layer composition was observed to take place during the first hours of immersion [14,15]. Saturated calomel electrode (SCE) was used as a reference electrode. A mesh of AISI 316 stainless steel that surrounds the working electrode acted as counter electrode. The sweeping rate of the potential was 0.17 mV/s, following the advice of the ASTM G61 standard. The current limit for reversing the sign of the potential sweep was 10^{-4} A/cm². The multiplicity of measurements (3-4) assures the reliability of the results.

For checking the effect of the corrugations, polarization studies were repeated. In these cases, the corrugated bars had been machined to cylinders and the surface of the cylinders had been ground to 320.

The morphology of the attack after the corrosion tests as well as the influence of the microstructure were studied by optical microscopy.

The semiconducting properties of the passive layer were measured using Mott-Schottky analysis. To obtain these results, capacities were measured at 1 kHz. Cathodic polarization was applied. The polarization swept from +600 to -1300 mV vs. SCE, with 5 mV/s scanning rate. The usual electrochemically or thermally forced generation of the passive layer was not used, but the passive layers were left to modify spontaneously along 48 h in the medium of study. Hence, as realistic as possible working conditions were favoured.

The electrochemical cell configuration used in Mott-Schottky studies was similar to that used in polarization curves, as well as the specimens used to study the behaviour of the corrugated

surface and the material at the core of the bars. The media considered also included non-carbonated and carbonated Ca(OH)₂ saturated solutions, yet always without chlorides. The number of measurement repetitions was four to assure the scientific relevance of the obtained results. Since this is a relatively new technique, carbon steel corrugated bars were included in this part of the study for comparison purposes.

3. Results and discussion

3.1. Local mechanic properties and micro structural characterization

The results of the localized micro hardness measurements corresponding to UH can be seen in Fig. 1. A clear parallelism can be observed between hardness and the results of tensile strength and yield strength obtained in more traditional tests (Table 2). The obtained UH results prove that the corrugations are always far harder than the core of the bars. Greater differences were observed between core and corrugation in HW grades than in CW grades. Small hardness difference was observed between HW and CW corrugations for the same type of stainless steel. On the other hand, the amount of plastic work (W_{plast}) is inversely related to hardness (Fig. 1b). Thus, corrugations (which are harder than cores) present lower W_{plast} values. The evolution of the other parameters obtained from UH measurements and non-plotted in the figure (indentation module, mechanical work and elastic work) confirm these trends.

Local differences regarding mechanical behaviour in the different areas of the corrugated bars can be explained by the differences observed between the microstructures of corrugations and cores. Corrugations always have smaller grain size than cores (Table 3).

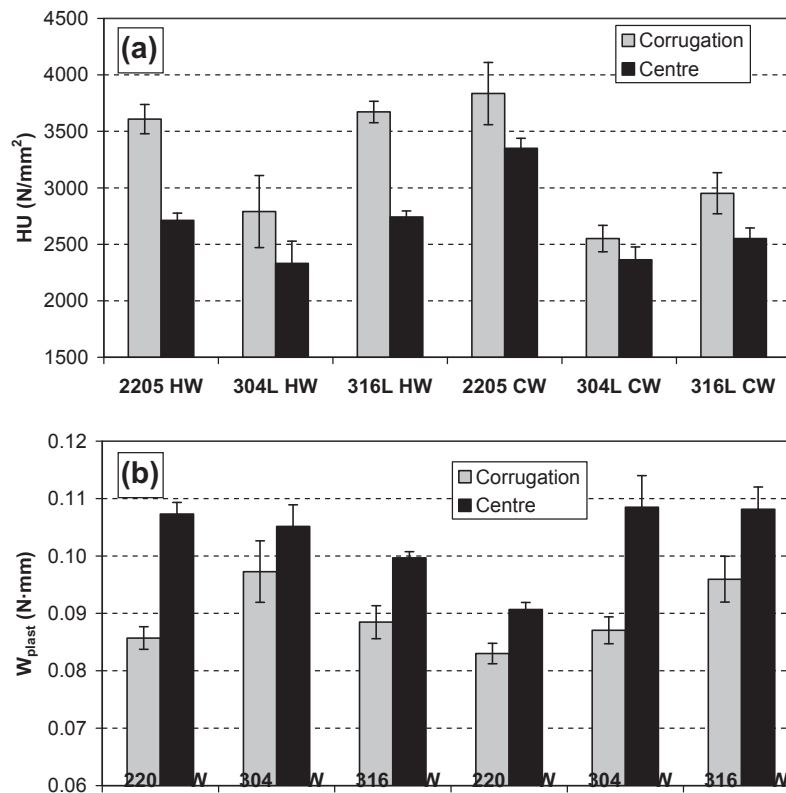
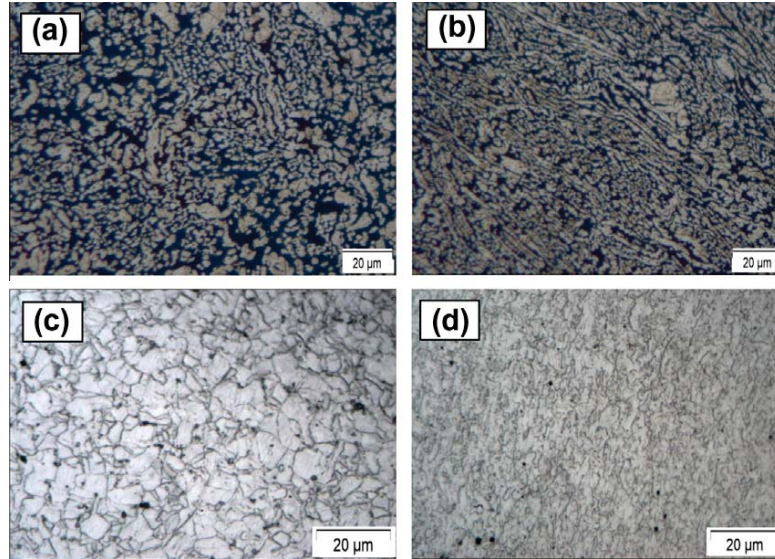


Fig. 1. Local mechanical properties measured on the corrugation and on the centre of the studied reinforcing stainless steels: (a) universal hardness (b) plastic work.

Table 3

Grain size on the corrugated surface and on the centre of the bar for the corrugated stainless steels considered in the study.

	AISI 304L		AISI 316L		SAF 2205	
	CW	HW	CW	HW	CW	HW
Grain size (μm)						
Corrugation	42 \pm 2	4.9 \pm 0.9	47 \pm 4	2.9 \pm 0.3	2.7 \pm 0.2	1.8 \pm 0.1
Centre	51 \pm 3	6.6 \pm 0.7	60 \pm 4	3.6 \pm 0.4	4.3 \pm 0.4	3.9 \pm 0.6

**Fig. 2.** Cross sectional views of the microstructure of the corrugated bars: (a) core of CW 2205 (b) outer region of CW 2205 (c) core of the HW 316L (d) outer region of the HW 316L.

This leads to lower hardness in the core than in the surface of the bars. HW grades have smaller grain size than CW. This smaller grain size explains the high yield strength of HW bars, in spite of being processed at high temperature (Table 2). Besides, a striking difference was observed between the grain sizes of austenitic and duplex bars. Because of their reduced grain size, the corrugated 2205 grades studied can be considered as microduplex (duplex with average austenite grain size between 5 and 16 μm) [33]. Microduplex stainless steels had been previously studied in the bibliography mainly because of their markedly superplastic behaviour at high temperatures [34].

Apart from the reduced grain size, deformation is another factor that contributes to the greater hardness measured in corrugations. Grain is more strained in the corrugations due to processing, which led to the accumulation of stresses in this area. This can be observed both in corrugated CW grades (Figs. 2a, b) and HW grades (Figs. 2c, d). The development of preferential texture in the corrugation (Figs. 2b, d) implies the formation of low atomic density planes in these regions. It has been suggested in literature that the lower binding energy of the atoms in this less close packed plane can result in enhanced diffusion rate for the atoms [19]. This fact might modify the characteristics of the passive layer in the corrugations.

3.2. Semiconducting properties of passive layers

The application of the Mott Schottky model to capacity (C) measurements of stainless steels informs about the semi conductive properties of oxides. The results presented in this work prove that the semi conductive properties of passive layers on

corrugated stainless steels are affected not only by base metal composition and medium features but also by material processing. The representation of C^{-2} vs. potential (E) obtained for the different stainless steels at frequencies dominated by the capacitive behaviour of the passive layer give rise to Mott Schottky plots as those in Figs. 3 and 4. At both pHs, two regions where C^{-2} varies linearly with the potential can be distinguished for all stainless steels. The negative slope at lower E corresponds to an oxide film that behaves as a p type semiconductor. A positive slope can be observed in the plots for medium E values, indicating that the passive layer also comprises an oxide films that behaves as an n type semiconductor. Both regions are separated by a narrow E range where the two oxides are in flat band conditions. This region of flat band condition appears at lower potentials as pH in the medium increases. Moreover, the behaviour of other n type semiconductor can be guessed at high anodic polarizations.

It is well known that passive films on stainless steels usually comprise an inner layer rich in Cr oxides and an outer layer rich in Fe oxides/hydroxides [35]. When the tests are carried out in carbon steel reinforcements, only the contribution of the n types oxides appear on the plot (Fig. 5). This fact proves, as other authors have also assumed before [23,35,36-38], that the oxides with n type behaviour are Fe oxides, while the p type behaviour corresponds to the Cr oxide. The presence of different Fe oxides in these alkaline conditions (Fe_3O_4 , Fe_2O_3 , etc.) [14] may explain the complex structure observed in the high E region of the plots.

The doping densities of the oxides was calculated using the Mott Schottky equation [35] and assuming a value for the relative dielectric constant (ϵ_r) of the films of 12, as it has been previously done by other authors [37,39]. The results on the doping density

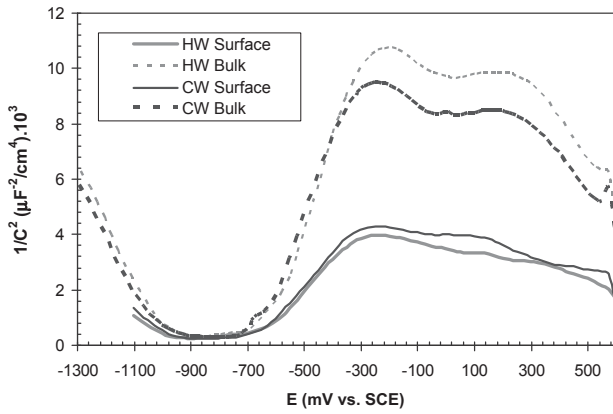


Fig. 3. Mott-Schottky plots for the passive layer formed on the corrugated surface and on the core of HW 2205 and CW 2205 in non-carbonated solutions.

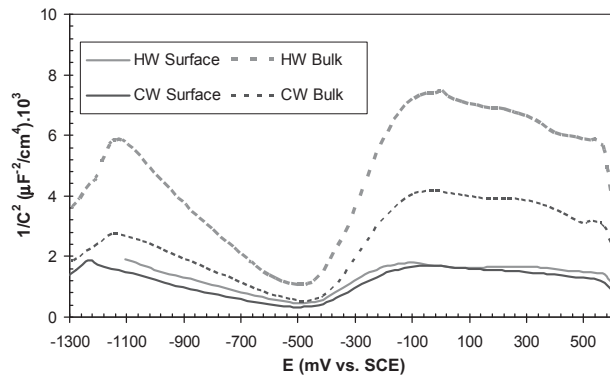


Fig. 4. Mott-Schottky plots for the passive layer formed on the corrugated surface and on the core of HW 2205 and CW 2205 in carbonated solutions.

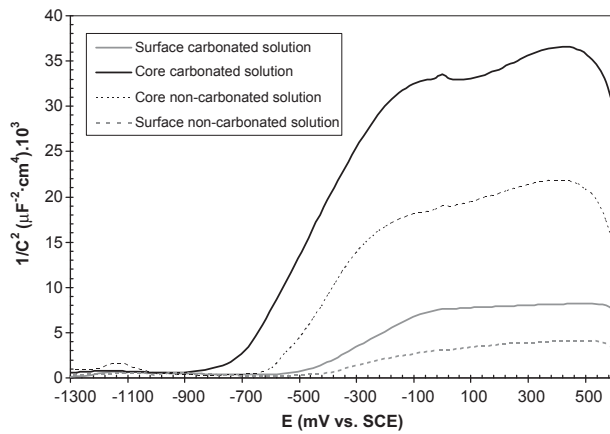


Fig. 5. Mott-Schottky plots corresponding to the passive layer on the corrugated surface and on specimens for the bulk of reinforcing black steel bars. The layers have spontaneously been formed in non-carbonated and carbonated solutions.

are shown in Table 4. In stainless steels, the density of donors in the structure of n type semiconductive oxides is determined from the slope observed in medium E . This density of dopants corresponds to oxygen vacancies that act as donors (N_d). n type semiconduction means that energy bands rise to the electrolyte

[35]. That is, increased N_d would favour, from the viewpoint of energy, the diffusion of aggressive anions such as Cl^- from the exterior to the base metal and the diffusion of metallic cations in the opposite direction. Both processes would favour corrosion. Besides, increased N_d has also been experimentally proven to lead to increased probability of pitting nucleation in passive layers generated in stainless steel, although in conditions different from those in the present study [20,39].

For stainless steel bars, N_d is always lower for specimens manufactured from the core of the bars than for those specimens of the same corrugated materials (Table 4). This would indicate that the Fe oxides appearing on corrugations are less protective than those forming on the core material in stainless steels. The lack of stoichiometry in oxides on the corrugations might well be related to the higher atomic disorder in the base metal shown in UH results (Fig. 1). On the contrary, the black oxide layer that appears on the surface of carbon steel bars during processing show more protective semiconductive properties than the passive layer formed in specimens for the core of the bar. When the corrugated black steel bars are exposed to simulated pore solutions, N_d is lower than N_d for the bulk material in the same conditions.

At first sight the high N_d values detected for duplex 2205 may well seem somewhat striking when compared to those measured for CW austenitic grades, when duplex is a better performing steel against corrosion [10]. In this case, influence from grain size (lower in duplex than in austenitic grades, as shown in Table 3) on oxide stoichiometry cannot be discarded. The higher Cr content in 2205 grades (Table 1), which provides passive layers with greater Cr_2O_3 [14], may also imply that Fe oxide stoichiometry in these grades becomes more conditioned by underlying Cr oxide stoichiometry than in austenitic grades.

In the studied stainless steel bars, the values of N_d show that the Fe oxides on the surface of HW grades have less oxygen vacancies than those on the surface of CW grades (Table 4). The greater oxide stoichiometry observed in HW grades may be related to the lower stresses and strains involved by this forming procedure.

N_d is also observed to decrease as pH becomes increasingly alkaline for the same material in both stainless and carbon steels (Table 4). These results are consistent with Thermodynamics, as the formation of (more stoichiometric) protective Fe oxides is more thermodynamically favoured by pH 12-13 than pH 9.

In the Cr oxide layer, stoichiometric deviations are cation vacancies that behave as acceptor dopants. Acceptor density (N_a) in Cr oxide was calculated from the slopes in the linear areas of the Mott-Schottky plots at low E . The penetration of aggressive ions with Cl^- is inhibited in p type oxides [35]. It has been said that pitting corrosion decreases as N_a increases in the oxides [20]. Table 4 shows that greater N_a tends to be observed for passive layers on corrugations than on bar core. The passivation treatment applied to the outer side of the corrugated bar, which favours Cr_2O_3 formation [14], could explain the higher N_a values for the corrugations. Other clear tendencies observed for Cr oxide in Table 4 include that: (a) greater N_a is observed in carbonated than in non-carbonated solutions, and (b) among CW processed bars, the 2205 grade has much higher N_a under all conditions than austenitic grades. This parallelism between N_d and N_a values in the passive layer is the expected in stainless steels with more than 15% Cr content [23,37]. The formation of Fe oxides and Cr oxides in the passive layer is obviously interrelated as well as that greater or lower stoichiometry in one of them definitely conditions the stoichiometry of the other.

The duplex structure in passive layers hinders the direct extrapolation of a relation between the conductivity of the passive layer in stainless steels and the susceptibility to pitting corrosion, because those factors that have a positive impact on the protective nature of Fe oxides affect the Cr oxides negatively. Previous works

	Centre		Corrug.		Centre		Corrug.		Centre		Corrug.	
	CW	HW	CW	HW	CW	HW	CW	HW	CW	HW	CW	HW
N_d in non-carbonated	1.6 ± 0.8	11.2 ± 2.1	9.2 ± 0.9	4.5 ± 0.1	5.1 ± 0.0	2.9 ± 0.8	6.3 ± 0.7	4.1 ± 0.7	3.3 ± 0.6	7.6 ± 0.9	3.9 ± 0.8	8.4 ± 1.1
N_a in non-carbonated	-	-	6.3 ± 0.4	4.9 ± 0.2	3.0 ± 0.0	2.7 ± 0.3	3.9 ± 0.4	3.5 ± 0.9	3.1 ± 0.2	14.6 ± 0.7	5.4 ± 0.8	12.4 ± 0.9
N_d in carbonated	5.8 ± 1.9	10.9 ± 3.2	18.7 ± 3.4	9.2 ± 1.1	10.8 ± 0.2	7.2 ± 0.1	30.1 ± 3.1	11.7 ± 1.4	8.9 ± 3.5	37.1 ± 7.2	8.9 ± 2.1	30.4 ± 5.3
N_a in carbonated	-	-	24.5 ± 3.9	16.3 ± 3.3	16.1 ± 2.0	15.8 ± 2.8	54.6 ± 5.1	23.5 ± 5.9	29.5 ± 2.6	48.9 ± 14.4	29.8 ± 0.5	37.0 ± 9.7

have shown that increased N_d has prevailing negative effect for the corrosion behaviour of a specific type of stainless steel under some specific conditions [38]. However, systematic negligence of the role of Cr oxides might be a big mistake. Besides, it must be taken into account that beyond oxide stoichiometry the thickness, exact composition and concentration of the different oxides in each layer

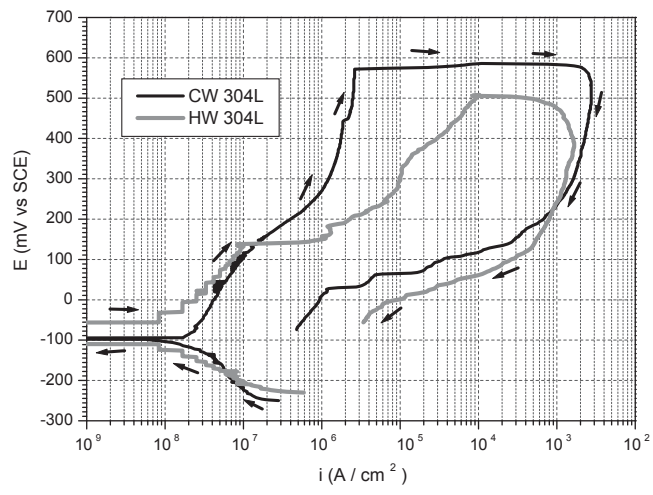


Fig. 6. Polarization curves for HW 304L and CW 304L in non-carbonated solution with 0.5% NaCl.

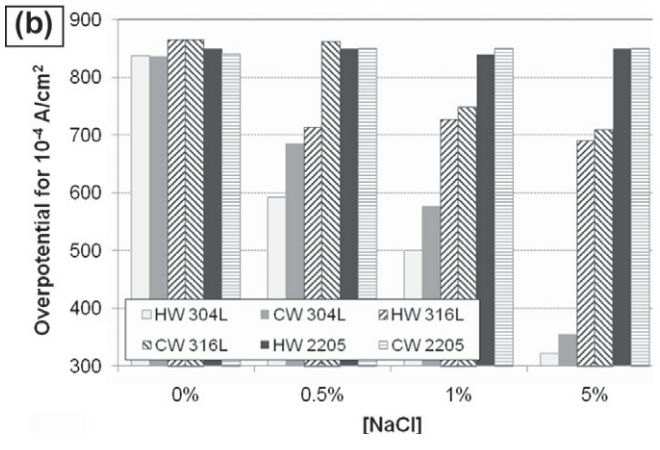
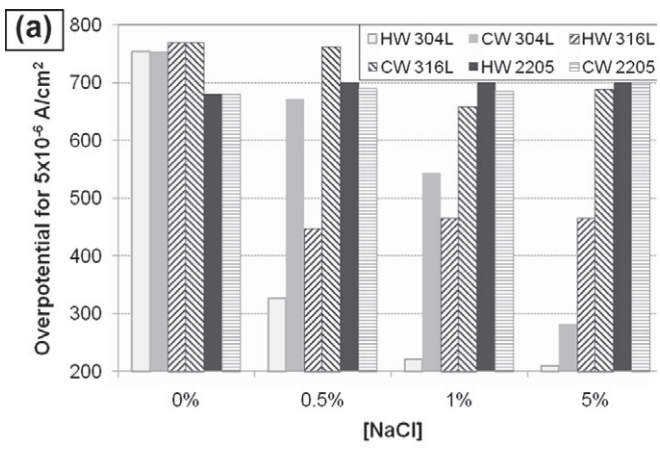


Fig. 7. Anodic overpotentials for the studied corrugated stainless steels in non-carbonated solutions: (a) for reaching $5 \times 10^{-6} \text{ A/cm}^2$; (b) for reaching 10^{-4} A/cm^2 .

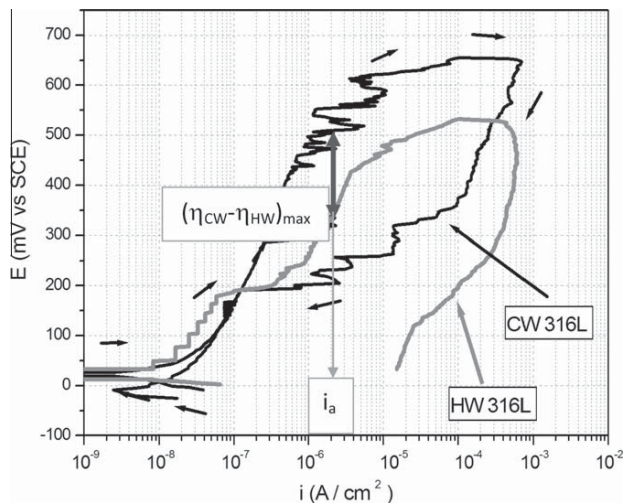


Fig. 8. Polarization curves for HW 316L and CW 316L in carbonated solutions with 0.5% NaCl.

is a key factor when it comes to determine its corrosion behaviour, as previously mentioned [14]. These other factors may well mask the relation between defect density in the oxides forming the passive layer and its stability in corrosive media [36].

The obtained results of the Mott Schottky analysis clearly prove that the stoichiometric features of the passive layers depend on stainless steel microstructure and processing. As it has been commented, a big amount of the previous research on the corrosion behaviour of stainless steels in concrete is carried out with stainless steels processed in a different way or with different surface finishing from reinforcing bars. Mott Schottky data suggest that the extrapolation from those results to the corrosion behaviour of corrugated stainless steels can be risky.

3.3. Behaviour to anodic polarization of corrugated surfaces

The polarization curves of corrugated austenitic steels in non carbonated $\text{Ca}(\text{OH})_2$ saturated solutions with different chloride content also show clear differences due to the forming process. As shown in Fig. 6, a well defined passive area and a clear pitting potential (E_p) can be observed in the anodic polarization curves for CW austenitic grades (in the case of 304L in non carbonated solutions containing 0.5% NaCl, E_p would be 560 mV vs. SCE). Once E_p is exceeded, current intensity increases very quickly in CW grades.

On the other hand, in HW austenitic grades, corrosion seems to begin at lower anodic overpotential, usually with scarcely defined E_p (in the case of HW 304L in non carbonated solutions containing 0.5% NaCl may be around 140 mV vs. SCE). However, the increases in corrosion intensity after the onset of the attack are milder than in CW austenitic grades.

The influence of the type of forming on corrosion behaviour can be ascertained by observing the data corresponding to the corrugated bars of types 304L and 316L in chloride containing solutions

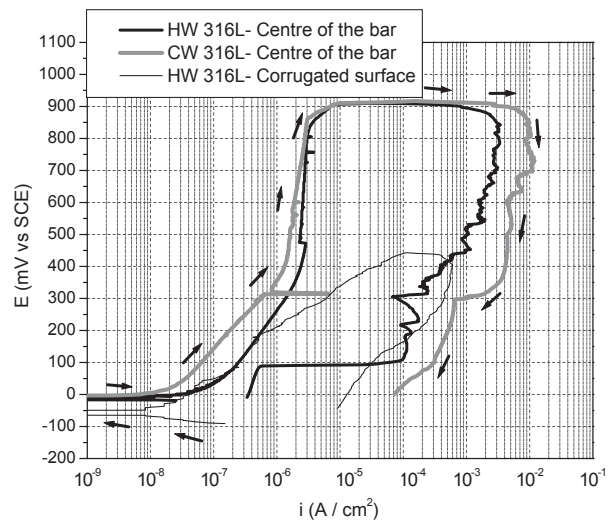


Fig. 9. Polarization curves for the cores of HW and CW 316L bars in carbonated solution with 1% NaCl. Curve corresponding to the corrugated surface of one of the materials in that media is included for comparison.

in Fig. 7. To reach current intensities around $5 \mu\text{A}/\text{cm}^2$, which characterize active corrosion (Fig. 7a), higher anodic overpotentials are reported in CW than in HW grades for the same austenitic types. That is, corrosive attack is more likely to begin in HW than in CW grades in aggressive media. If polarization continues, the differences observed between the overpotentials needed to reach a specific anodic current intensity decrease. This can be seen for the austenitic grades at $10^{-4} \text{ A}/\text{cm}^2$ (Fig. 7b) and becomes particularly clear at high chloride contents. The shape of the curves of CW and HW austenitic grades in low chloride concentrations suggests that the curves would intersect at anodic intensities higher than $10^{-4} \text{ A}/\text{cm}^2$. This points out that, although corrosion in CW grades requires more powerful corrosion cells to start than in HW grades with the same composition because their higher E_p , the attack in CW grades progresses more dangerously once it has started.

For non carbonated solutions without chlorides, the six materials are completely corrosion proof in the tests and the overpotentials represented in Fig. 7 correspond to reaction of decomposition of water. In these cases, the plotted overpotentials exhibit always similar values. However, the overpotentials of duplex grades at $5 \mu\text{A}/\text{cm}^2$ are an exception, being lower than those of the austenitic grades in the same conditions. Due to the higher Cr content of the duplex stainless steels (Table 1), oxidation from Cr(III) to Cr(VI) [12] is observed to contribute to a great extent to the anodic polarization curve in this area.

Duplex 2205 grades, regardless of chloride content of the medium and the forming method, were immune to corrosion in the performed tests. All the polarization curves obtained for 2205 are rather similar. This can be checked in the similarity of the data corresponding to HW and CW 2205 grades in Fig. 7a, b.

The influence of the forming conditions in carbonated media observed in austenitic grades is similar to that observed at higher pH levels (Fig. 8), but carbonation has a detrimental effect on the

Table 5

Parameters obtained from the polarization curves in carbonated, saturated $\text{Ca}(\text{OH})_2$ solutions with different chloride contents.

	AISI 304L			AISI 316L		
% NaCl	0.5	1	5	0.5	1	5
$\Delta(\eta_{\text{CW}} - \eta_{\text{HW}})_{\text{max}}$ (mV)	130	116	96	260	172	4
i_a (A/cm^2)	10^{-6}	6×10^{-8}	3×10^{-8}	1.3×10^{-6}	2×10^{-7}	1.3×10^{-7}

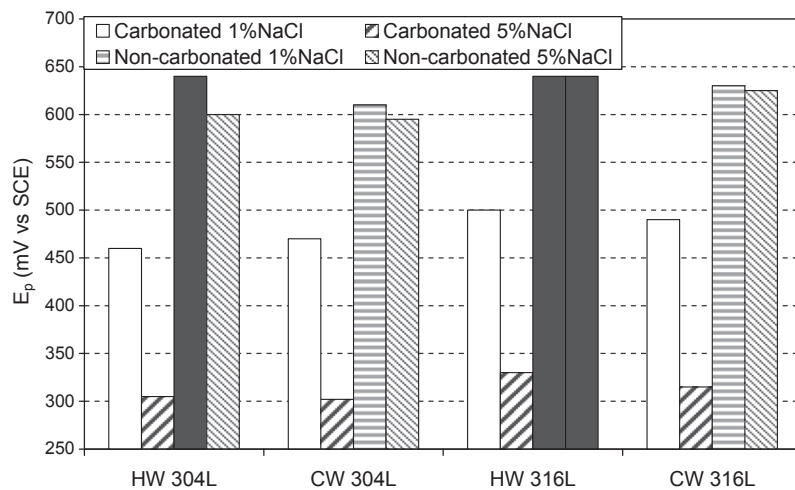


Fig. 10. E_p values obtained for the core of the bars in carbonated and non-carbonated solutions with chlorides. Black bars represent systems where water decomposition conditions are reached, and pitting does not take place.

corrosion behaviour of austenitic stainless steels as it has been observed and justified previously [10,14]. The onset of corrosion occurs at lower anodic overpotentials for HW grades. However, when corrosion appears in CW grades, it progresses quicker than in HW. For corrugated CW austenitic steels, within a specific intensity interval, the anodic overpotential needed to reach a certain intensity (η_{CW}) is always higher than that needed by HW bars with the same composition (η_{HW}). Table 5 shows the maximum differences between η_{CW} and η_{HW} reported by polarization curves of corrugated 304L and 316L in carbonated solutions, as well as the anodic intensity (i_a) at which the difference $\eta_{CW} - \eta_{HW}$ becomes maximum for each type of stainless steel and Cl^- concentration in the medium. In Fig. 8 both parameters are plotted.

Table 5 shows that the lower the aggressiveness of the medium is, the greater the influence of the forming conditions on the shape of the polarization curves is. This has been concluded from the fact that the parameter used to quantify the influence of the forming process $(\eta_{CW} - \eta_{HW})_{max}$ decreases as chloride content increases. Another outstanding fact is that these maximum differences between the HW and CW curves for the same grade appear at progressively lower i_a depending on chloride content, this corroborating the fact that these processing related differences could become less meaningful in highly aggressive media where highly powerful corrosion cells would appear.

In carbonated media the 2205 grade proves itself immune to corrosion under all studied conditions, regardless of its forming method.

3.4. Behaviour to anodic polarization of the bar cores

Different results are obtained when polarization curves are carried out in specimens machined from bar cores, whose microstructure clearly differs from that in bar surface (Table 2 and Fig. 3). An example of these differences between corrugated surface and core material is shown in Fig. 9. Corrosion resistance of bar cores is much greater than that of the corrugated surfaces of the same bars under the same conditions. Anodic polarization of both HW and CW bar cores always shows a clearly defined passive area and much higher E_p than those detected for corrugated surface. Several researches show that pitting onset can be directly related to the hardening processes occurring in the outer part of the bars (Fig. 1) [17,40]. This difference of behaviour between bar core

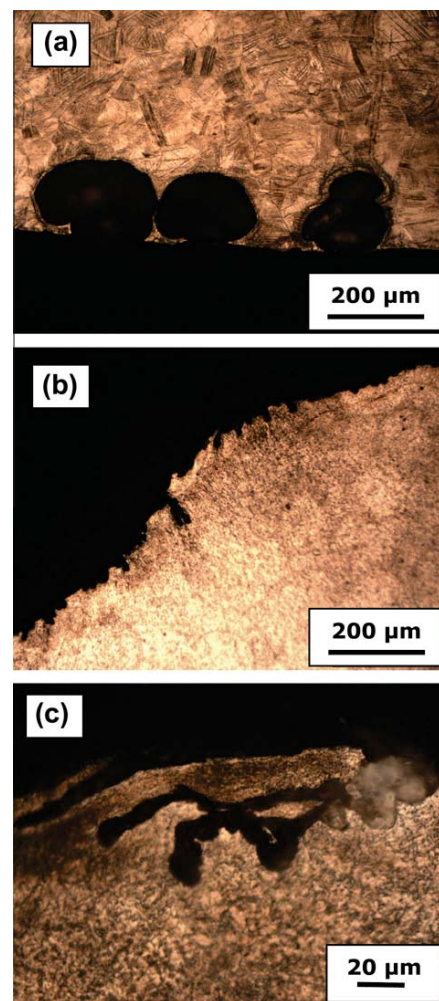


Fig. 11. Cross-sectional views of the morphology of the pits in corrugated surfaces after polarization in solutions with chlorides: (a) CW 304L; (b) HW 304L (predominant way of attack); (c) HW 304L (detail of the most strained region).

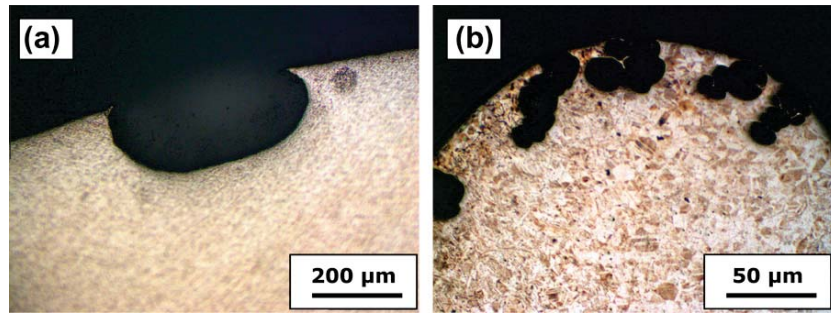


Fig. 12. Cross-sectional views of the morphology of the pits in specimens manufactured from the cores of the bars after polarization in solutions with chlorides: (a) HW 304L; (b) CW 304L.

and corrugation may also be related to the higher N_d values obtained for the passive layers formed in the corrugated surfaces of the cores of the same material under identical exposure conditions (Table 4). These data prove that the corrosion resistance of stainless steels in concrete may easily be overestimated when the specific features of the corrugations are not considered.

The E_p obtained from the polarization tests completed in the bar core of austenitic grades are shown in Fig. 10. It is important to highlight that the potentials corresponding to non carbonated solution of the HW 304L containing 1% NaCl and the HW 316L with 1% and 5% NaCl (black bars in the figure) do not correspond (because of the shape of the curves) to pitting corrosion processes but to water decomposition. That is, the materials plotted in black bars are immune to corrosion in the carried out tests. If E_p values are compared for the same stainless steel and medium composition, it can be observed that differences in the corrosion behaviour of HW and CW bar cores are smaller than those due to forming process when the study is completed on bar surface. Unlike corrugations, the forming method bears little significance in the corrosion behaviour of bar cores. However, results suggest that HW cores tend to be slightly more corrosion resistant than CW cores.

The present results suggest that the stoichiometric features of the Cr oxide (N_a) may have a significant impact on pitting onset, while attack speed may be influenced to a greater extent by Fe oxide stoichiometry (N_d). However, it seems rather obvious for stainless steels in alkaline media that no easily recognisable relationship between the results of capacity and corrosion behaviour studies can be obtained. It is due to the complex structure of the passive layers (formed by Cr and Fe oxides of changing nature and different thickness ratios depending on the base material and medium). The possible masking of the effect of stoichiometry on pitting behaviour by other characteristics of the passive layers should also be considered.

3.5. Study on attack morphology

The different shape of polarization curves depending on the microstructure of the corrugated bar corresponds to different attack morphologies. Thus, polarization of CW austenitic grades in media with chlorides, in both carbonated and non carbonated solutions, gives rise to the appearance of globular pitting on the bar surface (Fig. 11a). Pits tend to appear in the most strained area of the corrugations, characterized by greater stress (Fig. 1).

The prevailing attack morphology in austenitic HW is very small pits (Fig. 11b), that are numerous and well distributed on those areas with greater mechanic strains (Fig. 2d). This type of morphology explains the curve shape observed for HW grades (Figs. 6 and 8), where passive layer breakage does not lead to abruptly increas-

ing intensity, unlike it occurs with CW grades. The morphological study of the attack confirms that for HW grades, where corrosion develops for lower anodic overpotentials, attack tends to adopt a less aggressive mechanism. The greatest danger of localized vs. generalised corrosion becomes particularly relevant when dealing with concrete reinforcements. The tensile stresses created in concrete by localized corrosion of the reinforcements are far more dangerous than stresses created by uniform corrosion. The pressures to cause cracking of the concrete cover under non uniform corrosion conditions are proven to be much smaller than under uniform corrosion [41].

Another fact that can be drawn from the study of the morphology of the attack is that the shape of small pits in HW grades is often conditioned by microstructure deformation (Fig. 11c). It must also be pointed out that a few big pits, similar to those observed in CW grades, were also observed for HW austenitic grades after testing.

The pits caused by polarization tests in HW specimens machined from the bulk of austenitic bars clearly differ from those appearing on the surface of HW bars (Fig. 12a). After the polarization test, pits, when they appear, are large and exhibit globular shape. In samples manufactured from the core of CW austenitic grades, globular pits also appear, but in this case they develop in an interconnected way (Fig. 12b).

4. Conclusions

1. The forming process of the corrugations strongly modifies the microstructure of the stainless steels and it has an important effect on the characteristics of the passive layers and on the corrosion behaviour of the stainless steels.
2. The stoichiometry of the oxides that form the passive layers of the stainless steel corrugated bars is higher in the bar core than in the corrugated surface.
3. In the studied simulated pore solutions, CW bars have less stoichiometric passive layer than HW bars.
4. Cr and Fe oxides in the passive layer of stainless steels exhibit higher N_a and N_d , respectively, in carbonated than in non carbonated media.
5. The core of the corrugated bars presents much lower pitting probability than bar surface. Besides, the morphology of the anodic polarization induced attack is clearly different.
6. Less powerful corrosion cells are needed for corrosion onset in the corrugated surface of HW grades than in CW grades with identical composition.
7. If the attack of the corrugated surface starts in CW grades, it tends to develop in a more localised and faster manner than in the corrugated surface of HW grades.

Acknowledgement

The authors wish to acknowledge the Spanish Ministry of Science and Innovation (through project BIA2007 66491 C02 02) for its financial support in this research.

References

- [1] L.G. Andion, P. Garcés, F. Cases, C.G. Andreu, J.L. Vázquez, Metallic corrosion of steels embedded in calcium aluminate cement mortars, *Cem. Concr. Res.* 31 (2001) 431–436.
- [2] M.C. García-Alonso, M.L. Escudero, J.M. Miranda, M.I. Vega, F. Capilla, M.J. Correia, M. Salta, A. Bennani, J.A. González, Corrosion behaviour of new stainless steels reinforcing bars embedded in concrete, *Cem. Concr. Res.* 37 (2007) 1463–1471.
- [3] M. Criado, D.M. Bastidas, S. Fajardo, A. Fernández-Jiménez, J.M. Bastidas, Corrosion behaviour of a new low-nickel stainless steel embedded in activated fly ash mortars, *Cement Concr. Compos.* 22 (2011) 644–652.
- [4] U. Nürberger (Ed.), *Stainless steel in concrete. State of the art report*, Publication n° 18, Institute of Materials, London, 1996.
- [5] M.F. Hurley, J.R. Scully, Threshold chloride concentration of selected corrosion-resistant rebar materials compared to carbon steel, *Corrosion* 62 (2006) 892–904.
- [6] Guidance on the use of stainless steel reinforcement, Technical report N° 51, The Concrete Society, London, 1998.
- [7] H. Castro, C. Rodríguez, F.J. Belzunce, A.F. Cantelli, Mechanical properties and corrosion behaviour of stainless steel reinforcing bars, in: T.R. Torralba (Ed.), *New Developments on Metals*, Vol. III, 2Color SL, Madrid, 2001, pp. 81–86.
- [8] H. Castro, C. Rodríguez, F.J. Belzunce, A.F. Cantelli, Mechanical properties and corrosion behaviour of stainless steel reinforcing bars, *J. Mater. Process. Technol.* 143–144 (2003) 134–137.
- [9] L. Freire, M.J. Carmezim, M.G.S. Ferreira, M.F. Montemor, The passive behaviour of AISI 316L in alkaline media and the effect of pH: A combined electrochemical and analytical study, *Electrochim. Acta* 55 (2010) 6174–6181.
- [10] A. Bautista, G. Blanco, F. Velasco, Corrosion behaviour of low-nickel austenitic stainless steels reinforcements: A comparative study in simulated pore solutions, *Cem. Concr. Res.* 36 (2006) 1922–1930.
- [11] M. Kouril, P. Novak, M. Bojko, Threshold chloride concentration for stainless steels activation in concrete pore solutions, *Cem. Concr. Res.* 40 (2010) 431–436.
- [12] S.M. Alvarez, A. Bautista, F. Velasco, Corrosion behaviour of corrugated lean duplex stainless steels in simulated pore solutions, *Corros. Sci.* 53 (2011) 1748–1755.
- [13] L. Bertolini, F. Bolzoni, T. Pastore, P. Pedferri, Behaviour of stainless steel in simulated concrete pore solution, *Br. Corros. J.* 31 (1996) 218–222.
- [14] A. Bautista, G. Blanco, F. Velasco, A. Gutiérrez, L. Soriano, F.J. Palomares, H. Takenouti, Changes in the passive layer of corrugated, low-Ni, austenitic stainless steel due to the exposure to simulated pore solutions, *Corros. Sci.* 51 (2009) 785–792.
- [15] A. Bautista, G. Blanco, H. Takenouti, EIS study of passivation of austenitic and duplex stainless steels reinforcements in simulated pore solutions, *Cement Concr. Compos.* 28 (2006) 212–219.
- [16] A. Bautista, G. Blanco, F. Velasco, M.A. Martínez, Corrosion performance of welded stainless steels reinforcements in simulated pore solutions, *Constr. Build. Mater.* 21 (2007) 1267–1276.
- [17] K.R. Trethewey, M. Wenman, P. Chard-Tuckey, B. Roebuck, Correlation of meso- and micro-scale hardness measurements with pitting of plastically deformed Type 304L stainless steel, *Corros. Sci.* 50 (2008) 1132–1141.
- [18] U. Kamachi Mudali, P. Shankar, S. Ningshen, R.K. Dayal, H.S. Khatak, B. Raj, On the pitting corrosion resistance of nitrogen alloyed cold worked austenitic stainless steels, *Corros. Sci.* 44 (2002) 2183–2198.
- [19] A. Barbucci, G. Cerisola, P.L. Cabot, Effect of cold-working in the passive behavior of 304L stainless steel in sulfate media, *J. Electrochem. Soc.* 149 (2002) B534–B542.
- [20] G. Bianchi, A. Cerquetti, F. Mazza, S. Torchio, Electronic properties of oxide films and pitting susceptibility of type 304L stainless steel, *Corros. Sci.* 12 (1972) 495–502.
- [21] M.J. Carmezim, A.M. Simoes, M.F. Montemor, M. Da Cunha Belo, Capacitance behaviour of passive films on ferritic and austenitic stainless steel, *Corros. Sci.* 47 (2005) 581–591.
- [22] A. Fattah-Alhosseini, M.A. Golozar, A. Saatchi, K. Raeissi, Effect of solution concentration on semiconducting properties of passive films formed on austenitic stainless steels, *Corros. Sci.* 52 (2010) 205–209.
- [23] N.E. Hakiki, B. Maachi, F. Mechehoud, C. Pirri, A. Mehdaoui, J.L. Bubendorff, *Structural and Semiconductive Investigation of Passive Films and Thermally Grown Oxides on Stainless Steels*, Paper 58, 7th European Stainless Steel Conference, Como (Italy) September 2011.
- [24] C.M. Abreu, M.J. Cristobal, R. Losada, X.R. Novoa, G. Pena, M.C. Pérez, Long-term behaviour of AISI 304L passive layer in chloride containing medium, *Electrochim. Acta* 51 (2006) 1881–1890.
- [25] M. Abreu, M.J. Cristobal, R. Losada, X.R. Novoa, G. Pena, M.C. Pérez, The effect of Ni in the electrochemical properties of oxide layers grown on stainless steels, *Electrochim. Acta* 51 (2006) 2991–3000.
- [26] L. Freire, X.R. Novoa, G. Pena, V. Vivier, On the corrosion mechanism of AISI 204Cu stainless steel in chlorinated alkaline media, *Corros. Sci.* 50 (2008) 3205–3212.
- [27] M. Kouril, P. Novak, M. Bojko, Limitations of the linear polarization method to determine stainless steel corrosion rate in concrete environment, *Cement Concr. Compos.* 28 (2006) 220–225.
- [28] L. Veleva, M.A. Alpuche-Avilés, M.K. Graves-Brook, D.O. Wipf, Voltammetry and surface analysis of AISI 316L stainless steel in chloride-containing simulated concrete pore environment, *J. Electroanal. Chem.* 578 (2005) 45–53.
- [29] B. Elsener, D. Addari, S. Coray, A. Rossi, Nickel-free manganese bearing stainless steel in alkaline media – Electrochemistry and surface chemistry, *Electrochim. Acta* 45 (2011) 4489–4497.
- [30] S. Fajardo, D.M. Bastidas, M. Criado, M. Romero, J.M. Bastidas, Corrosion behaviour of a new low-nickel stainless steel in saturated calcium hydroxide solution, *Constr. Build. Mater.* 25 (2011) 4190–4196.
- [31] A. Iversen, B. Leffler, Aqueous corrosion of stainless steel, in: B. Cottis, M. Graham, R. Lindsay, S. Lyon, T. Richardson, D. Scantlebury, H. Stott (Eds.), *Shreir's Corrosion*, vol. 3, Elsevier, Amsterdam, 2010, pp. 1802–1878.
- [32] F. Velasco, G. Blanco, A. Bautista, M.A. Martínez, Effect of welding on local mechanical properties of stainless steels for concrete structures using universal hardness tests, *Constr. Build. Mater.* 23 (2009) 1883–1891.
- [33] G. Lothongkim, P. Wongpanya, S. Morito, T. Furuhashi, T. Maki, Effect of nitrogen on corrosion behaviour of 28Cr-7Ni duplex stainless steels in air-saturated 3.5wt% NaCl solution, *Corros. Sci.* 48 (2006) 137–153.
- [34] N. Orhan, T.I. Kahn, M. Eroglu, Diffusion bonding of a microduplex stainless steel next term to Ti-6Al-4V, *Scripta Mater.* 45 (2001) 441–446.
- [35] S. Fujimoto, H. Tsuchiya, Semiconductor property of passive films and corrosion behavior of Fe-Cr alloys, in: Y. Waseda, S. Suzuki (Eds.), *Characterization of Corrosion Products on Steel Surfaces*, Springer, Berlin Heidelberg, 2006, pp. 33–49.
- [36] L.V. Taveira, M.F. Montemor, M. Da Cunha Belo, M.G. Ferreira, L.F.P. Dick, Influence of incorporated Mo and Nb on the Mott-Schottky behaviour of anodic films formed on AISI 304L, *Corros. Sci.* 52 (2010) 2813–2818.
- [37] N.E. Hakiki, S. Boudin, B. Rondot, M. Da Cunha Belo, The electronic structure of passive films formed on stainless steels, *Corros. Sci.* 37 (1995) 1809–1822.
- [38] S. Ningshen, U. Kamachi Mudali, V.K. Mittal, H.S. Khatak, Semiconducting and passive films properties of nitrogen-containing type 316LN stainless steel, *Corros. Sci.* 49 (2007) 481–496.
- [39] J.-B. Lee, S.-I. Yoon, Effect of nitrogen alloying on the semiconducting properties of passive films and metastable pitting susceptibility of 316L and 316LN stainless steels, *Mater. Chem. Phys.* 122 (2010) 194–199.
- [40] L. Peguet, B. Malki, B. Baroux, Influence of cold working on the pitting corrosion resistance of stainless steel, *Corros. Sci.* 49 (2007) 1933–1948.
- [41] B.S. Jang, B.H. Oh, Effects of non-uniform corrosion on the cracking and service life of reinforced concrete structures, *Cem. Concr. Res.* 40 (2010) 1441–1450.